



## Influence of activated sludge characteristics on membrane fouling in a hybrid membrane bioreactor

Xiaochang C. Wang<sup>a,\*</sup>, Yisong S. Hu<sup>a</sup>, Qiang Liu<sup>b</sup>

<sup>a</sup>Key Lab of Northwest Water Resource, Environment and Ecology, MOE, Xi'an University of Architecture and Technology, Xi'an 710055 China  
Tel. +86 29 8220 2125; Fax: +86 29 8552 2471; email: xcvwang@xauat.edu.cn  
<sup>b</sup>Xuzhou Institute of Technology, Xuzhou 221008, China

Received 20 October 2010; Accepted 31 March 2011

### ABSTRACT

A pilot study was conducted in a domestic wastewater treatment plant for investigating the behaviour of a hybrid membrane bioreactor (HMBR) which was developed by adding biofilm carriers into a conventional membrane bioreactor (CMBR). As a result of long term operation, the HMBR performed organic, nitrogen and phosphorous removal much better than the CMBR under the same operation condition. The HMBR also showed a better property of membrane fouling control as it could be continuously operated without washing or chemical cleaning for about 140 d till the trans-membrane pressure (TMP) reached the prescribed value of 20 kPa while the continuous operation period for the CMBR was about 60 d. Investigations were further conducted on the characteristics of the activated sludge in the reactors regarding biomass quantity, SVI, particle size distribution, sludge particle structure and supernatant turbidity. It was found that the addition of biofilm carriers not only brought about a substantial increase of biomass quantity due to the growth of attached biomass, but also an improvement of the structure, size, flocculability and settleability of the sludge particles. A cake layer resistance model was developed to simulate the process of TMP increase in the cake layer forming stage. It was evaluated that the specific resistance of the cake layer in the case of the HMBR would only be 1/4 of that in the case of the CMBR.

*Keywords:* Hybrid membrane bioreactor; Biofilm carrier; Activated sludge; Membrane fouling; Particle size distribution; Cake layer resistance

### 1. Introduction

In recent years there are increasing interests in using membrane bioreactor (MBR) for wastewater treatment and reclamation. However, membrane fouling becomes the main obstacle to restrict the wide application of MBR [1,2]. Many studies by far have focused on membrane fouling control. In the author's previous study [3], a hybrid membrane bioreactor (HMBR) was developed by introducing biofilm carriers into the reactor. Due to

the simultaneous existence of suspended and attached biomasses, the HMBR showed its advantage over the conventional membrane bioreactor (CMBR) in both contaminant removal and membrane fouling control. Sombatsompop et al. also reported the characteristics of the attached biomass in an MBR as its better oxygen transfer, higher nitrification/denitrification effect and biomass concentration, more effective organic removal, and slower membrane fouling rate [4].

Membrane fouling in an MBR may be determined by many factors such as the membrane properties [5], the hydrodynamic environment in the reactor [6], and

\*Corresponding author.

the characteristics of the activated sludge in the mixed liquor [7]. As membrane fouling is a result of the interaction between the membrane and the mixed liquor [8], the activated sludge characteristics would affect largely the membrane's performance. Membrane fouling is phenomenally evident as a rise in the trans-membrane pressure (TMP). The fouling history can be described as TMP rise in several stages, such as an initial short-term rapid rise in TMP followed by a long-term weak rise in TMP, and finally a TMP jump [5,7,9]. The long-term gradual increase in TMP is often closely related to the growth of a cake layer on the membrane surface which can contribute up to 80% of the filtration resistance [10]. As the cake layer on the membrane surface is considered to be formed by the deposited particles from the mixed liquor, the activated sludge characteristics in the mixed liquor should greatly affect the cake layer property and its resistance to filtration.

With these in mind, the authors tried to compare the performance of the HMBR with a conventional membrane bioreactor (CMBR) under the same operation condition. Attention was paid to the influence of activated sludge characteristics on the cake layer resistance in the two reactors.

## 2. Materials and methods

### 2.1. Raw wastewater characteristics

The experimental work for this study was conducted using a pair of pilot scale membrane bioreactors installed at a domestic wastewater treatment plant in Xi'an, China. The raw wastewater, after flowing through a sand settler and a coarse screen, was fed to the pilot MBRs as the influent. Its quality during the experimental period is shown in Table 1.

### 2.2. Experimental set-up and operational conditions

Fig. 1 is the schematic diagram of the pilot systems used in this study. It consisted of a rectangular aeration tank equipped with a submerged PVDF hollow fibre micro-filtration (MF) membrane module (pore size 0.2  $\mu\text{m}$ , Tianjin Motimo Membrane Technology Ltd.) and associated pumping, aerating, flowrate control and measurement devices. The aeration tank was partitioned by a perforated wall into two rooms, one for aeration and another for accommodating the membrane module.

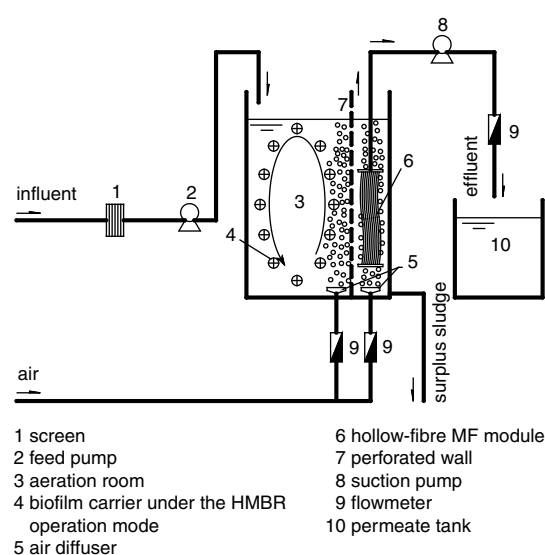


Fig. 1. Schematic diagram of the pilot system.

The aeration room could perform the function of a conventional reactor without addition of biofilm carriers, or the function of a hybrid reactor when biofilm carriers (Kaldnes K3, AnoxKaldnes Corporation, Norway) were added. The former was the operation mode of a conventional membrane bioreactor (CMBR) and the later was the operation mode of a hybrid membrane bioreactor (HMBR). The membrane room was also equipped with air diffusers at its bottom for providing shear force on the submerged membrane for fouling control.

Table 2 shows the operation condition of the pilot systems under the CMBR and HMBR operation modes. All the operational parameters were almost identical for the CMBR and HMBR, except for the increase of total biomass for the HMBR due to attached biomass formation on the biofilm carriers. In the whole process of experimental operation the membrane flux was maintained constantly at 10  $\text{l m}^{-2} \cdot \text{h}^{-1}$ . The suction pump was operated in intermittent on/off cycles (on: 8 min; off: 2 min) to assist membrane fouling control. Chemical cleaning was conducted only when the trans-membrane pressure (TMP) reached a prescribed maximum value of 20 kPa.

### 2.3. Chemical analysis

Chemical analysis in this study was conducted regarding COD, TP, TN and  $\text{NH}_4\text{-N}$  of the influent

Table 1  
Influent quality to the pilot MBRs

COD ( $\text{mg l}^{-1}$ )	BOD <sub>5</sub> ( $\text{mg l}^{-1}$ )	$\text{NH}_4^+\text{-N}$ ( $\text{mg l}^{-1}$ )	TN ( $\text{mg l}^{-1}$ )	TP ( $\text{mg l}^{-1}$ )	TSS ( $\text{mg l}^{-1}$ )	pH	Temperature ( $^{\circ}\text{C}$ )
240–896	185–423	20.3–46.8	22.5–54.1	4.3–13.2	200–1210	7.0–7.5	13.1–25.7

Table 2  
Operation condition of the pilot systems

Reactor	Membrane flux ( $1 \text{ m}^{-2} \cdot \text{h}^{-1}$ )	Suspended biomass (MLSS) ( $\text{mg l}^{-1}$ )	Attached biomass ( $\text{mg l}^{-1}$ )	Total biomass ( $\text{mg l}^{-1}$ )
CMBR	10	3850–4248 (4058)	0	3850–4248 (4058)
HMBR	10	3810–4350 (4021)	1605–1750 (1687)	5415–6100 (5708)

Note: Value in the brackets as the average.

and effluent of the pilot system. The methods utilised include: dichromate method for COD, ammonium molybdate spectrophotometric method for TP, alkaline potassium persulphate digestion-UV spectrophotometric method for TN, and Nessler's reagent colorimetric method for  $\text{NH}_4\text{-N}$ .

#### 2.4. Characterization of the physical properties of the activated sludge

In this study, supernatant turbidity of the mixed liquor from the aeration room was used as a parameter to characterize the flocculability of the activated sludge. The sludge volume index (SVI) was used as a parameter to characterize the settleability of the activated sludge. The appearance of the sludge particles were observed using an optimal microscope (BX60, Olympus) equipped with a digital camera (Infinity 3, Olympus), and the size distribution of the sludge particles was analyzed using a laser granularity distribution analyzer (LS 230/SVM+, Coulter, USA).

The suspended biomass was characterized by MLSS in the aeration room, and the attached biomass was analyzed by direct measurement of the attached solid weight following Luostarinen et al. [11].

#### 2.5. Cake layer resistance model for characterizing the pressure increase during filtration

In order to characterize the dynamic variation of membrane resistance that brings about a continuous increase of TMP under the condition of constant flux filtration for both the CMBR and HMBR, a mathematical model was developed as below.

According to Darcy's law, the relationship between the flux and TMP during membrane filtration can be expressed as:

$$J = \frac{\Delta p}{\mu(R_m + R_c)} \quad (1)$$

where  $J$  = membrane flux;  $\Delta p$  = pressure drop across the membrane (TMP);  $\mu$  = absolute viscosity;  $R_m$  = intrinsic membrane resistance;  $R_c$  = cake layer resistance. In the filtration process the accumulation of materials on the

membrane over time produces an increase in  $R_c$  and  $R_m$  over time. In the case where  $R_c$  is dominated by the formation of a cake of constant resistance per unit depth, and membrane resistance is constant over time,  $R_c$  can be expressed as:

$$R_c = \hat{R}_c \delta_c \quad (2)$$

where  $\hat{R}_c$  = specific resistance of the cake;  $\delta_c$  = thickness of the cake. The change in cake thickness with time can be expressed by the following differential equation [12]:

$$\frac{\partial \delta_c}{\partial t} = k_1 J - k_2 \delta_c \quad (3)$$

where  $k_1$  = the rate constant of forward-transport of cake-forming materials to the membrane, while  $k_2$  = the rate constant of back-transport of materials from the membrane.

Eq. 3 can be rewritten to the following form if  $k_1$ ,  $k_2$  and  $J$  are time independent:

$$\frac{d\delta_c}{dt} + k_2 \delta_c = k_1 J \quad (4)$$

By integrating Eq. (4) with an initial condition of  $\delta_c = 0$  as  $t = t_0$ , the following result can be obtained:

$$\delta_c = \frac{k_1 J}{k_2} (1 - e^{-k_2(t-t_0)} \cdot e^{-k_2 t_0}) \quad (5)$$

Substituting Eq. (5) into Eqs. (2) and (1) and solving it for  $\Delta p$ , we get:

$$\Delta p = \mu J R_m + \mu J^2 \hat{R}_c \frac{k_1}{k_2} (1 - e^{-k_2 t_0} \cdot e^{-k_2 t}) \quad (6)$$

or

$$\Delta p = \Delta p_0 + A(1 - B \cdot e^{-k_2 t}) \quad (7)$$

where  $\Delta p_0$  = pressure drop due to the intrinsic membrane resistance;  $A$  = coefficient related to the specific cake resistance, forward-transport rate and back-transport rate;  $B$  = coefficient related to the back-transport rate. Equations (6) and (7) are used in this study for comparing the cake resistances between the CMBR and HMBR.

### 3. Results and discussion

#### 3.1. TMP increase in the CMBR and HMBR

As shown in Fig. 2, a continuous TMP increase was observed under constant flux filtration for both the CMBR and HMBR. In the case of the CMBR, the time for TMP to reach the prescribed maximum value of 20 kPa was about 60 d, while in the case of the HMBR, it was prolonged to about 140 d. Although only two cycles operation was conducted for each of the reactors in the current study, it was seen that TMP could almost return to the initial value after chemical cleaning and the length of the second cycle was about the same as the first cycle. Even for the CMBR, the cycle length of 60 d was rather a long duration for continuous filtration without backwashing. The air scouring provided in the membrane room and the intermittent on/off operation of the suction pump were recognized to be effective ways for extending the working cycle.

#### 3.2. Contaminant removal by the CMBR and HMBR

The efficiency of contaminant removal by the CMBR and HMBR was compared regarding organics (COD), nitrogen ( $\text{NH}_4\text{-N}$  and TN) and phosphorus (TP). As shown in Fig. 3, although very good COD removal was performed by both reactors, the COD removal by the HMBR (95.0%) was apparently higher than that by the CMBR (90.4%). Regarding  $\text{NH}_4\text{-N}$  (Fig. 4), there was also a noticeable difference between its removal by the HMBR (98.8%) and that by the CMBR (93.3%). Similar tendencies were found for TN and TP as shown in Fig. 5 and Fig. 6, respectively, where their removals were 52.6%

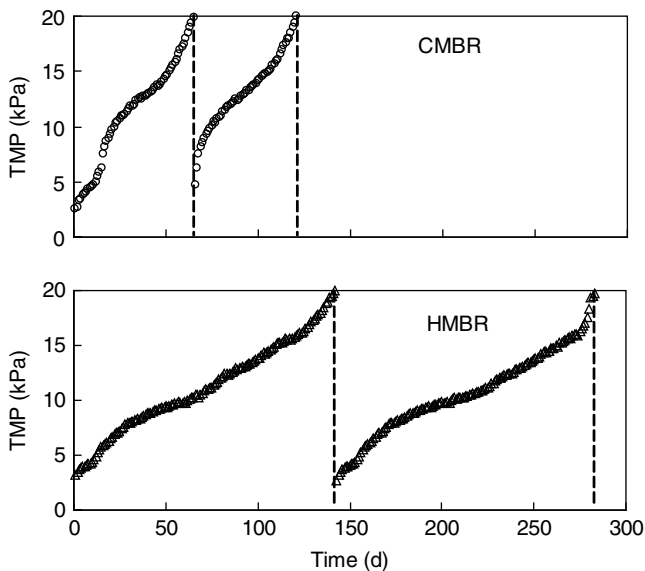


Fig. 2. TMP increase in the CMBR and HMBR.

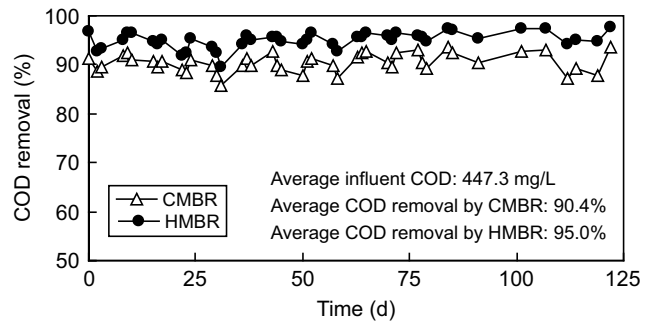


Fig. 3. COD removal by the CMBR and HMBR.

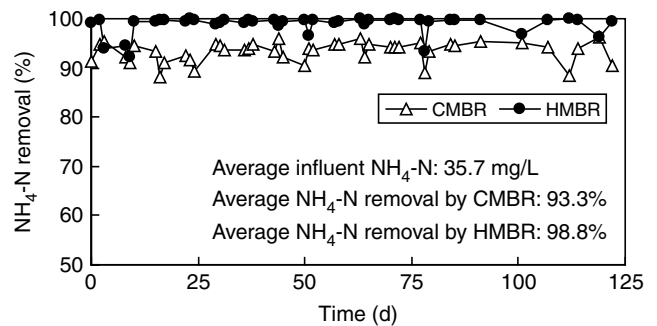


Fig. 4. Ammonia nitrogen removal by the CMBR and HMBR.

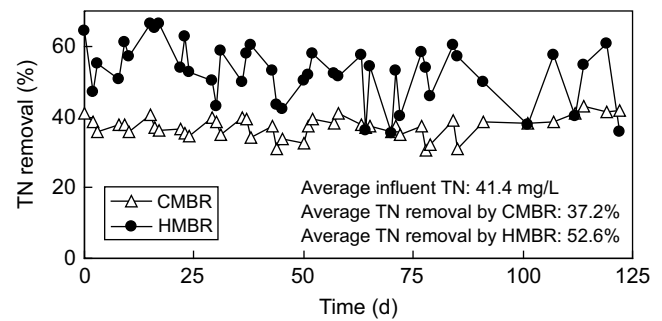


Fig. 5. Total nitrogen removal by the CMBR and HMBR.

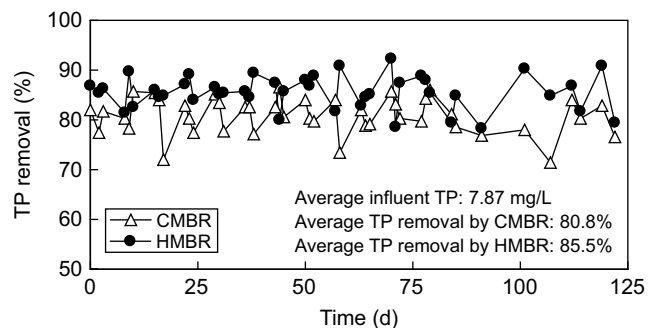


Fig. 6. Total phosphorous removal by the CMBR and HMBR.

and 85.5% by the HMBR versus 37.2% and 80.8% by the CMBR. The much better effect of the HMBR for contaminant removal may be attributed to the higher quantity of biomass in the reactor than the CMBR (Table 1), and due to the simultaneous existence of suspended and attached biomasses in the HMBR, nitrification and denitrification effect may be much improved [13].

### 3.3. Physical characteristics of activated sludge in the CMBR and HMBR

During the pilot experiments, samples of mixed liquor were collected from both the CMBR and HMBR for analyses regarding particle appearance and size distribution, supernatant turbidity after settling, and sludge volume index (SVI). Generally speaking, the sludge particles from the CMBR appeared smaller and looser as a result of microscopic observation. Fig. 7 shows the representative graphs of a number of sludge samples regarding the particle size distribution in the CMBR and HMBR. The average diameter of the particles from the CMBR was 29.32  $\mu\text{m}$  while that from the HMBR was much larger as 56.8  $\mu\text{m}$ . Another characteristic of the particle size distribution was that the uniformity of the particles, if expressed as the ratio of  $d_{90}/d_{10}$  where  $d_{90}$  and  $d_{10}$  are the diameters corresponding to 90% and 10% accumulative volumes, respectively, were significantly

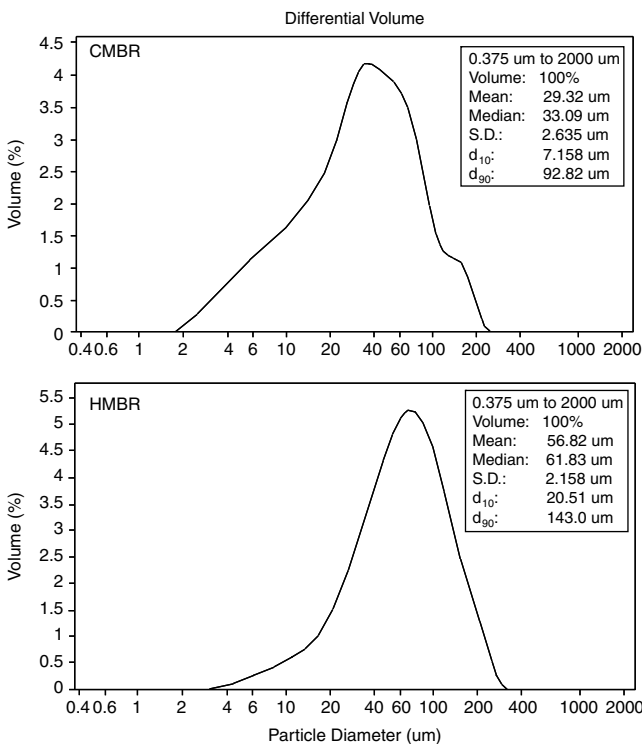


Fig. 7. Representative graphs of the size distribution of the activated sludge particles in the CMBR and HMBR.

different between the CMBR and HMBR:  $d_{90}/d_{10} = 12.97$  for the CMBR and  $d_{90}/d_{10} = 6.97$  for the HMBR. It indicated that the activated sludge particles in the HMBR were in a much narrower size range.

The supernatant turbidity shown in Fig. 8 could be taken as another factor to indicate the flocculability of the sludge floc for fine particles. The lower NTU of the supernatant from the HMBR (6.1 NTU on average) than that from the CMBR (8.3 NTU on average) was an indication of better flocculability. The much lower SVI of the sludge from the HMBR (128  $\text{ml g}^{-1}$  on average) than that from the CMBR (201  $\text{ml g}^{-1}$  on average) as shown in Fig. 9 indicated that the HMBR operation resulted in the formation of flocs with much better settlability and more compact structure.

### 3.4. Comparison of the cake layer resistances in the CMBR and HMBR

Fig. 10 was plotted using the data measured within one cycle of operation for both the CMBR and HMBR. From the tendency of the measured TMP variation with time, the following phenomena are noticeable:

1. In the case of the CMBR, TMP increased rapidly from the beginning of the filtration cycle following an exponential manner, that is gradual deceleration of

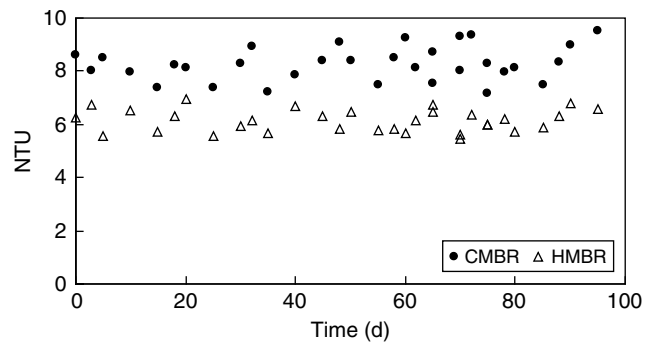


Fig. 8. Supernatant turbidity in the CMBR and HMBR.

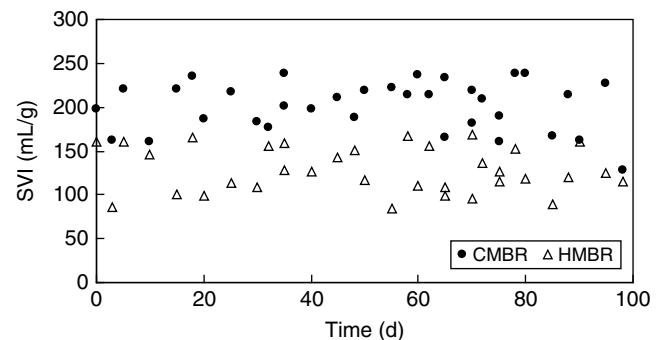


Fig. 9. SVI of the activated sludge in the CMBR and HMBR.

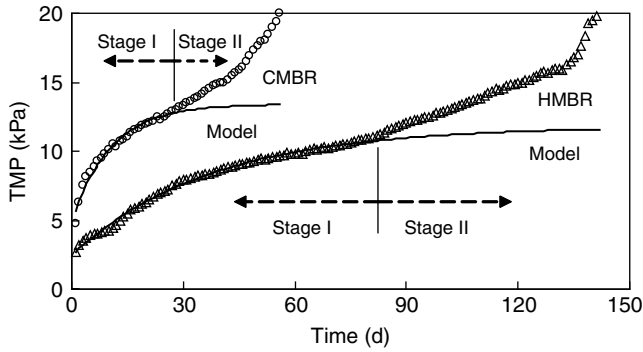


Fig. 10. Fitting of the cake layer resistance model with TMP data.

the rate of TMP rise until  $t = 30$  d, while in the case of the HMBR, TMP rise was much slower but still followed the exponential manner until  $t = 80$  d.

- From  $t = 30$  d in the case of the CMBR and  $t = 80$  d in the case of the HMBR, an inflection point could be found from each of the measured curves where the rate of TMP rise began to accelerate until it reached the prescribed maximum value of  $\text{TMP} = 20$  kPa.

It could thus be considered that the TMP rise with time experienced two stages, that is Stage I and Stage II with division at the inflection point (Fig. 10). By applying Eq. (7), that is the cake layer resistance model to Stage I in each case, a result was obtained as shown in Table 3 where  $A$ ,  $B$ , and  $k_2$  were parameters of the model curves that best fitted the measured TMP data. It can be seen in Fig. 10 that each of the model curves fitted the measured data in Stage I very well.

Of the parameters in Table 3,  $\mu$  and  $J$  were constants. If we further suppose that  $k_1$ , the rate constant of transport of cake-forming materials to the membrane would not differ much between the CMBR and HMBR due to similar hydrodynamic conditions, the relative magnitudes of the specific resistance of cake layers in the two reactors could be evaluated by a simple relation of:

$$\frac{[\hat{R}_c]_{\text{CMBR}}}{[\hat{R}_c]_{\text{HMBR}}} = \frac{[A \cdot k_2]_{\text{CMBR}}}{[A \cdot k_2]_{\text{HMBR}}} \quad (8)$$

Substituting the values of  $A$  and  $k_2$  for the CMBR and those for the HMBR into Eq. (8), we have:

$$\frac{[\hat{R}_c]_{\text{CMBR}}}{[\hat{R}_c]_{\text{HMBR}}} = 4.08 \quad (9)$$

It shows that the specific resistance of cake layer in the CMBR would be four times of that in the HMBR.

### 3.5. Influence of activated sludge characteristics on membrane fouling in the CMBR and HMBR

According to the Kozeny equation, the specific resistance of an incompressible cake composed of uniform particles can be calculated as [12]:

$$\hat{R}_c = \frac{180(1 - \epsilon_c)^2}{d_p^2 \epsilon_c^3} \quad (10)$$

where  $\epsilon_c$  = porosity of the cake;  $d_p$  = diameter of particles deposited. Although Eq. (10) cannot be directly used in this study because the activated sludge flocs were not uniform particles, it still explains that cake porosity and particle diameter are important factors affecting the specific resistance of cake layer. With larger floc diameters in the HMBR than that in the CMBR (mean particle size as  $56.82 \mu\text{m}$  vs.  $29.32 \mu\text{m}$  as shown in Fig. 7), the specific resistance of cake layer formed in the HMBR should be much smaller than that in the CMBR. On the other hand, because particles with more uniform size distribution often have larger void space between them when they are randomly piled up than particles of wider size range, the porosity of the cake may also be affected by the uniformity of the particles. The cake layer in the case of the HMBR may have larger porosity due to the deposition of more uniform particles, bringing about a reduction of the specific resistance.

The above discussion is based on an assumption that cake layer resistance is dominant in the filtration process, that is Stage I shown in Fig. 10. However, when filtration is prolonged to Stage II, the TMP rise will no longer follow the cake layer resistance model but begin to accelerate. Such a phenomenon has been explained as TMP

Table 3  
Parameters of the cake layer resistance model for the CMBR and HMBR

Parameter	Data range	$\Delta p_0$	$A = \mu J^2 \hat{R}_c \frac{k_1}{k_2}$	$B = e^{-k_2 t_0}$	$k_2$	Correlative coefficient
CMBR	$t < 30$ d	2.34	11.07	0.765	0.094	0.9769
HMBR	$t < 80$ d	2.34	9.45	0.988	0.027	0.9953

Note:  $\Delta p_0$  was measured as the TMP of clean membrane.

jump as the consequence of severe membrane fouling [5,14]. Comparing with other researchers' observation [7], the TMP jump depicted in Fig. 10 was not so "abrupt" or "sudden" but lasted for longer time in this study.

From a practical viewpoint, it may be strategically suggestible that the operation condition of an MBR should be controlled within the stage where cake layer resistance is dominant. As shown in Fig. 10, for the CMBR this stage can last for about 30 d with TMP below 13 kPa, while for the HMBR it can last for up to 80 d with TMP below 11 kPa. Because cake layer is often considered to belong to removable fouling [5], an MBR controlled in such an operation manner may effectively extend the lifetime of the membrane and reduce operation and maintenance costs.

#### 4. Conclusions

From this study, the following conclusions could be drawn:

1. In comparison with a conventional membrane bioreactor (CMBR), the hybrid membrane bioreactor (HMBR) with coexistence of suspended biomass in the mixed liquor and attached biomass on the biofilm carriers could effectively enhance organic removal, nitrification and denitrification, as well as phosphorus removal in the reactor. The operation cycle of the HMBR could be prolonged to about 140 d before TMP reached the prescribed maximum value comparing with about 60 d for the CMBR under similar operational condition.
2. In the HMBR the activated sludge particles in the mixed liquor that are the deposited materials to form a cake layer on the membrane surface were found to be larger and with narrower size distribution, better flocculability for fine particles, and better settleability than the particles in the CMBR. With these advantageous physical characteristics, the fouling control property was effectively improved.
3. The TMP rise within one operation cycle in either the CMBR or HMBR underwent two stages: Stage I featured by gradual TMP rise with decelerated rate and Stage II featured by quicker TMP rise with accelerated rate. Stage I could be mathematically depicted by a cake layer resistance model which was developed by introducing the rate of cake thickness variation into Darcy's law. By fitting the model with TMP data, it was evaluated that the specific resistance of cake in the CMBR would be four times of that in the HMBR. This may be attributed to the advantageous physical characteristics of the activated sludge particles in the HMBR.

#### Acknowledgements

This study is supported by the National Natural Science Foundation of China (Grant No. 50838005), the Program for Changjiang Scholars and Innovative Research Team in University (Grant No. IRT0853), and the National Program of Water Pollution Control (Grant No. 2008ZX07317-004).

#### References

- [1] C. Huyskens, E. Brauns, E.V. Hoof and H.D. Wever, A new method for the evaluation of the reversible and irreversible fouling propensity of MBR mixed liquor, *J. Membr. Sci.*, 323 (2008) 185–192.
- [2] F.G. Meng and F.L. Yang, Fouling mechanisms of deflocculated sludge, normal sludge, and bulking sludge in membrane bioreactor, *J. Membr. Sci.*, 305 (2007) 48–56.
- [3] B. Cao, X.C. Wang and E.R. Wang, A hybrid submerged membrane bioreactor process for municipal wastewater treatment and reuse. In Wang, X.C. and Chen, R. (Editors): *future of Urban Wastewater Systems—Decentralisation and Reuse*. China Building and Architecture Press, Beijing, (2005) 487–492.
- [4] K. Sombatsompop, C. Visvanathan and R. Ben Aim, Evaluation of biofouling phenomenon in suspended and attached growth membrane bioreactor systems, *Desalination*, 201 (2006) 138–149.
- [5] F. Meng, S.-R. Chae, A. Drews, M. Kraume and H.-S. Shin, Recent advances in membrane bioreactors (MBRs): Membrane fouling and membrane material, *Water Res.*, 43 (2009) 1489–1512.
- [6] A.P.S. Yeo, A.W.K. Law and A.G. Fane, Factors affecting the performance of a submerged hollow fibre bundle, *J. Membr. Sci.*, 280 (2006) 969–982.
- [7] J. Zhang, H.C. Chua, J. Zhou and A.G. Fane, Factors affecting the membrane performance in submerged membrane bioreactors, *J. Membr. Sci.*, 284 (2006) 54–66.
- [8] S. Rosemberger, H. Evenblij, S. te Poele, T. Wintgens and C. Laabs, The importance of liquid phase analyses to understand fouling in membrane assisted activated sludge processes—six case studies of different European research groups, *J. Membr. Sci.*, 263 (2005) 113–126.
- [9] B.D. Cho and A.G. Fane, Fouling transients in nominally sub-critical flux operation of a membrane bioreactor, *J. Membr. Sci.*, 209 (2002), 391–403.
- [10] J. Lee, W.-Y. Ahn and C.H. Lee, Comparison of the filtration characteristics between attached and suspended growth microorganisms in submerged membrane bioreactor, *Water Res.*, 35 (2001) 2435–2445.
- [11] S. Luostarinen, S. Luste, L. Valentin and J. Rintala, Nitrogen removal from on-site treated anaerobic effluents using intermittently aerated moving bed biofilm reactors at low temperatures, *Water Res.*, 40 (2006) 1607–1615.
- [12] M.R. Wiesner and P. Aptel, Mass transport and permeate flux and fouling in pressure-driven processes. In Mallevialle, J., Odendaal, P.E., Wiesner M.R. (Editors): *Water Treatment Membrane Processes*. McGraw-Hill, New York. (1996).
- [13] P. Artiga, V. Oyanedel and J.M. Garrido, An innovative biofilm-suspended biomass hybrid membrane bioreactor for wastewater treatment, *Desalination*, 179 (2005) 171–179.
- [14] A. Pollice, A. Brookes, B. Jefferson and S. Judd, Sub-critical flux fouling in membrane bioreactors—a review of recent literature, *Desalination*, 174 (2005) 221–230.